SPATIO-TEMPORAL DATA ANALYSIS WITH NON-LINEAR FILTERS: BRAIN MAPPING WITH *fMRI* DATA

Karsten RODENACKER, Klaus HAHN, Gerhard WINKLER, Dorothea P. AUER[1]

GSF-National Research Centre for Environment and Health,
Institute of Biomathematics and Biometry, Neuherberg, Germany
[1]Max-Planck-Institute for Psychiatry, NMR, München, Germany

ABSTRACT

Spatio-temporal digital data from fMRI (*functional Magnetic Resonance Imaging*) are used to analyse and to model brain activation. To map brain functions, a well-defined sensory activation is offered to a test person and the hemodynamic response to neuronal activity is studied. This so-called BOLD effect in fMRI is typically small and characterised by a very low signal to noise ratio. Hence the activation is repeated and the three dimensional signal (multi-slice 2D) is gathered during relatively long time ranges (3-5 min). From the noisy and distorted spatio-temporal signal the expected response has to be filtered out. Presented methods of spatio-temporal signal processing base on non-linear concepts of data reconstruction and filters of mathematical morphology (e.g. alternating sequential morphological filters). Filters applied are compared by classifications of activations.

Keywords: brain mapping, functional magnetic resonance imaging, non-linear filtering, mathematical morphology, spatio-temporal image analysis.

INTRODUCTION

Functional magnetic resonance imaging (fMRI) is a non-invasive method to get insight into the functioning of the brain. Sensory activation can be traced by the hemodynamic response to neuronal activity. This response, the blood oxygen level dependent effect, is typically very small and strongly distorted by noise in the same order of magnitude as the signal itself. Problems and proceedings of detecting such activated regions, hence the reproducible recognition of regions (volumes) with the expected response, are outlined in Fig. 1. A sketch of the BOLD-effect related to an activation is shown in Fig. 2. The distortion of the signals is the reason that activation patterns are repeated to allow a better correlation to the response. From this noisy and distorted spatial-temporal signal the expected response has to be filtered out. Applied methods of signal processing base on non-linear concepts of data reconstruction and recently developed filters of mathematical morphology (e.g. alternating sequential morphological filters). The proceeding of data analysis is shown in Fig. 3.

DATA ACQUISITION AND MATERIAL

Physiology

Upon neuronal activation, oxygen consumption, blood flow and volume locally increase to meet the higher metabolic demand of neuronal tissue. The rise in blood flow is disproportionally larger than the oxygen consumption, probably due to limited oxygen transport across capillaries. This results in a net increase in capillary and venous blood oxygenation, that can be measured by a special MR method, the so-called BOLD (blood oxygenation level

dependant, Ogawa et al., 1990) technique. BOLD contrast is generated by susceptibility or T2*- sensitive sequences that exploit the different magnetic properties of deoxyhemoglobin (DeoxHb, paramagnetic) and oxyhemoglobin (OxHb, diamagnetic), in that a reciprocal relationship exists between concentration of DeoxHb and observed signal intensity. Local signal increase of BOLD-fMRI in response to a neuronal stimulus therefore, reflects a rise in the OxHb to DeoxHb ratio and represents a non-invasive, yet indirect measure of neuronal activity.

fMRI was performed on a 1.5T Signa Echospeed (GE Medical Systems, Milwaukee) clinical scanner using the standard quadrature head coil. Multi-slice (7) single-shot gradient-echo echoplanar images (TR= 3000 ms, TE= 60 ms, flip angle = 90°) were acquired from the visual cortex during the visual stimulation period. Three on and four off periods (10 images each) were collected resulting in a time-series of 70 images and a temporal resolution of 3s. Nominal spatial resolution was 2.9x2.9x5 mm.

The visual stimulation was triggered with the MR acquisition and consisted of an 4 Hz alternating checkerboard projected onto a screen in front of the magnet bore that could be viewed by the subject through a mirror system.

Data processing: To compensate motion artefacts, images were rigidly realigned using the AIR algorithm (Woods et al., 1998, AIR 3.08).

The pattern of stimuli is outlined in Fig. 2. Response signals in a 3x3x1 neighbourhood are displayed in Fig. 4 (top left). After subtraction of the estimated linear trend (Fig. 4 top right), the resulting signals are outlined in Fig. 4 (lower left). The presented data stem from a visual experiment, however the method presented is applicable to any activation type.

Functional maps

To calculate functional maps, a segmentation of activated from non-activated areas is performed on the basis of the time course of signal intensity, applying various statistical methods. Commonly, split t-test, cross-correlation to an ideal reference waveform or Fourier analysis are used to pixelwise map statistical values. The next step is to define an appropriate cut-off and superimpose only thresholded pixels on a high resolution anatomical MRI, thus producing the 'functional map'.

Several methods exist to reconstruct the true data. Typical methods in brain mapping base on assumptions that smoothing methods compress the noisy input to feature or parameter maps for further discrimination or segmentation (methods of statistical parameter mapping (SPM)). The approach reported tries to transform the input data directly in the spatio-temporal domain by transformation(s). Non-linear Gaussian filters and filter chains as well as methods derived from mathematical morphology are applied and compared.

METHODS

Non-linear Gaussian filter and filter chains

The filter used is known as *sigma* filter. The noisy function is convoluted by the product of two Gaussian functions weighting the spatial and intensity spread.

$$NLG_{\sigma,\zeta} f(p) = \frac{1}{N} \sum_{q \approx p} g_{\sigma}(\|q-p\|) g_{\zeta}(|f(q)-f(p)|) f(q)$$

with $g_{\lambda}(t) = \exp\left(-\frac{t^2}{2\lambda^2}\right)$ and $N = \sum_{q} g_{\sigma}(\|q-p\|) g_{\zeta}(|f(q)-f(p)|)$ for normalisation purposes.

The sequential application of this filter:

$$f_{aus} = NLG_{\sigma_k,\zeta_k} \circ \ldots \circ NLG_{\sigma_1,\zeta_1}(f)$$

with increasing spatial width (σ) and decreasing intensity width (ζ)

$\sigma_1 =$ voxel width; $\sigma_{j+1} = \alpha \cdot \sigma_j$ and

$\zeta_1 = 3 \cdot STD$ of intensities; $\zeta_{j+1} = \frac{1}{\alpha}\zeta_j$; z.B. $\alpha = 2$

is the so-called Aurich chain, see (Aurich, 1998 and Winkler et al., 1999).

Sequential alternating filters from openings and closings in mathematical morphology

With $A, B \subset Z^n; 0 \in B$, B the structuring element and A the set or function. A weighted structuring element (*val(B)*) can be applied to functions.

Dilation: $C = A \oplus B = \bigcup_{b \in B} (A)_b = \bigcup_{b \in B} (A + val(B))_b$

Opening: $C = A_B = (A \ominus B) \oplus B$

Openclose: $C = (A^B)_B$

are shortly and not exactly defined (see for complete descriptions Serra, 1986, Sternberg, 1986 and Heijmans, 1995). The complementary functions like *erosion*, *closing* and *closeopen* are defined accordingly. A separate class of filters are *the alternating sequential morphological filter*:

$$C = (((...(A^{B_1})_{B_1})^{B_2})_{B_2})...)^{B_n})_{B_n} \; ; \; B_1 \subset B_2 \subset ... \subset B_n$$

They appear similar to the above outlined Aurich chain, although without the decreasing intensity spread. However the weighted structuring elements, applicable for functions, are similar to the Aurich chain in a certain extent.

The application of filters from the field of mathematical morphology on discrete time functions is shown in Fig. 5, 6 for different structuring elements with differing weighting functions. The structuring elements with their weights in the time domain are displayed beside the graphs. Two thick plotted lines show the filter results. The thin line represents the mean of the two complementary filters. This illustrates the behaviour of these filters on functions which is not widely used. Fig. 5 shows opening and closing with differently weighted structuring elements and Fig. 6 the results of *openclose* and *closeopen*.

Test scheme for classification

To evaluate or compare the filter results a classifier is implemented to test the existence of the activation pattern by several minimum maximum comparisons at certain adequate time intervals. This simple classifier does not replace an in-depth analysis using SPM or other tools for statistical analysis and discrimination. Its only purpose is to detect possible activation and to illustrate filter results.

EXAMPLES

Several filters and filter configurations are tested with varying parameters. Depending on the models applied (defined by the filter or structuring element sizes and shapes) the results are considerably controllable. This can be recognised in filter results shown in Fig. 4 and Fig. 5. The actually filtered signals used for classification could not be displayed due to the limited space.

Non-linear Gaussian filter and filter chain

In Fig. 7 one section is shown with classification results for increasing spread of the spatial Gaussian. The increased spread σ of the Gaussian stabilise the activation and reduces for higher spread the detection of artefacts.

Sequential alternating filters

Fig. 8 shows similar to fig. 7 the classification results for increasing spatial sizes of the structuring element with flat (unweighted) kernel in temporal dimension.

SUMMARY AND DISCUSSION

The application and test of spatio-temporal filters is, beside the problems concerning the necessary computing time, not trivial. The response as well as the distortions of the data are influenced by many different sources. The two approaches can roughly be characterised like follows:

Non-linear Gaussian filter and filter chain

- Modelling based on assumptions about the noise, less *a priori* knowledge for data necessary/possible
- Model often very simple (e.g. piece-wise constant function for the Aurich chain)
- Scaleability very good
- Relatively high amount of computing time

Mathematical morphology

- Modelling of the data, more *a priori* knowledge for data necessary
- Modelling by set oriented methods arbitrarily complicated
- Relatively little amount of computing time

The choice of method depends on the amount of knowledge available. Pre-processing can improve results of elaborated post-processing steps, e.g. SPM (statistical parameter mapping), considerably. However an objective evaluation of the methods is very difficult because of the number of unknown variants, the missing knowledge about the noise function(s), but also by the lack of adequate representation methods for visualisation of higher dimensional (> 2) data.

REFERENCES

Aurich V., Mühlhaus E., Grundmann S., Kantenerhaltende Glättung von Volumendaten bei sehr geringem Signal-Rausch-Verhältnis, 2. Aachener Workshop über Bildverarbeitung in der Medizin, 1998

Serra J., Image Analysis and Mathematical Morphology, Academic Press, London, 1982

Sternberg S.R., Grayscale Morphology, Computer Vision. Graphics and Image Processing, 33, 333-355, 1986

Heijmans, H.J.A.M., Mathematical Morphology: Basic Principles, Summer School, Zakopane, Poland, 1995

Ogawa S, Lee TM, Kay AR, Tank. Proc Natl Acad Sci USA 87:9868-72, 1990

Woods R.P., JCAT; 22: 155-165, 1998

Winkler, G., Aurich, V., Hahn, K., Martin, A., Rodenacker, K. Noise Reduction in Images: Some Recent Edge-Preserving Methods, Pattern Recognition and Image Analysis: Advances in Mathematical Theory and Applications, in press, 1999

Fig. 1: fMRI from the brain

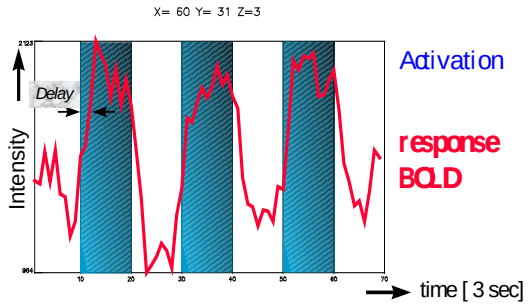

Fig. 2: BOLD Effect

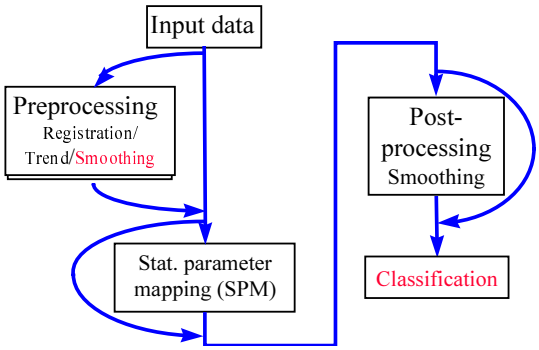

Fig. 3: Proceeding

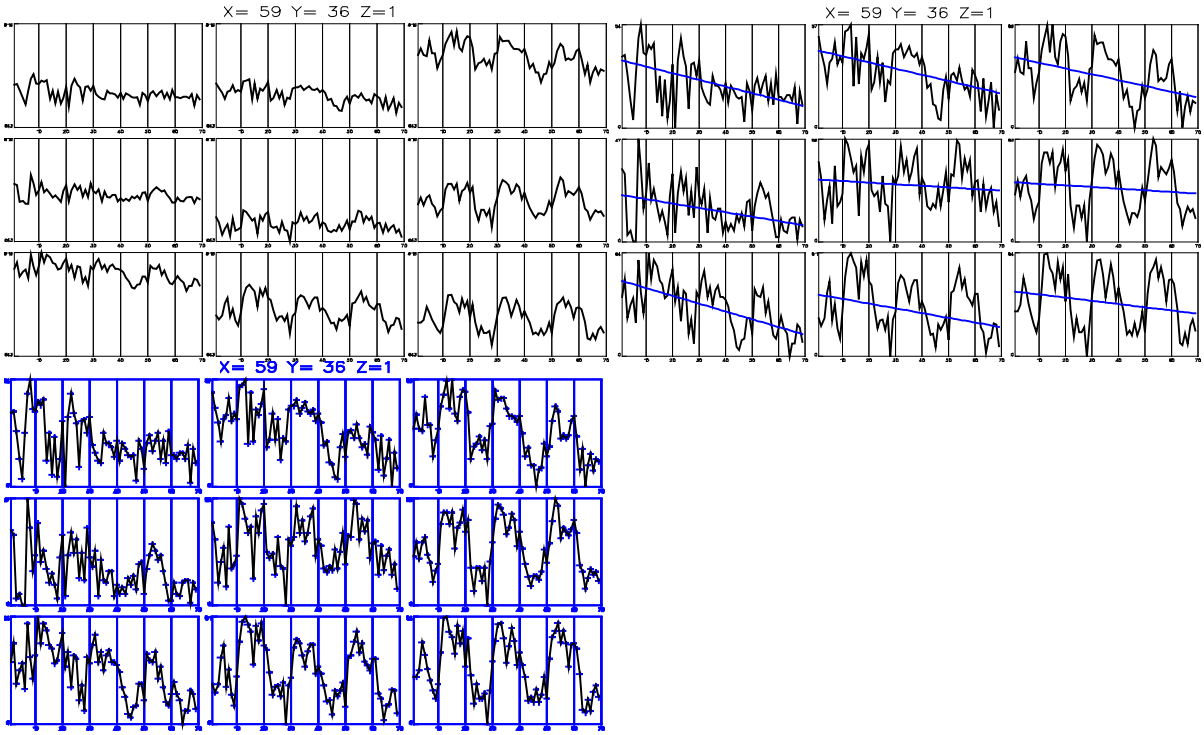

Fig 4: Data example, time signals in a 3x3x1 neighbourhood with trend elimination
trend elimination

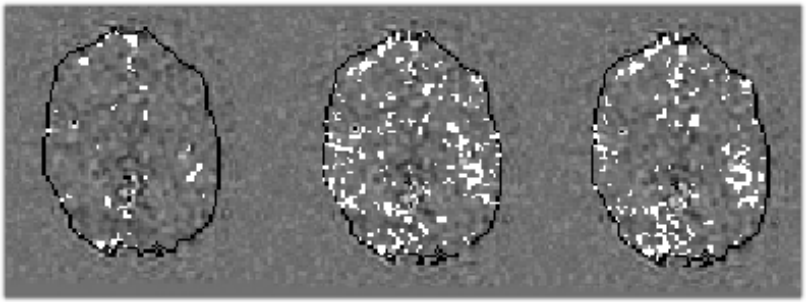

Fig. 7: Classification of Aurich chain transformed sections with σ = 1, 2, 4

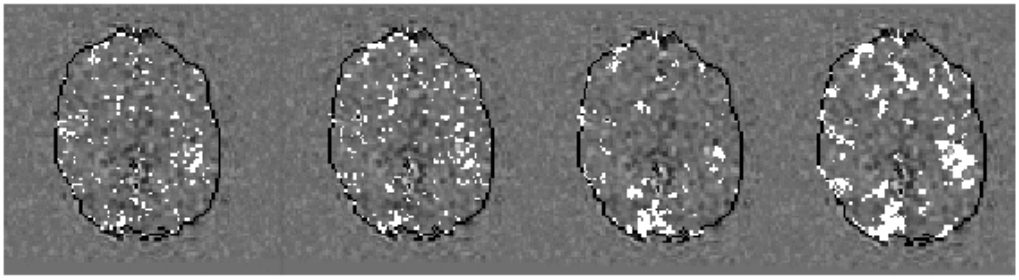

Fig. 8: Classifcation of morphological filter results by increasing sizes of structuring elements

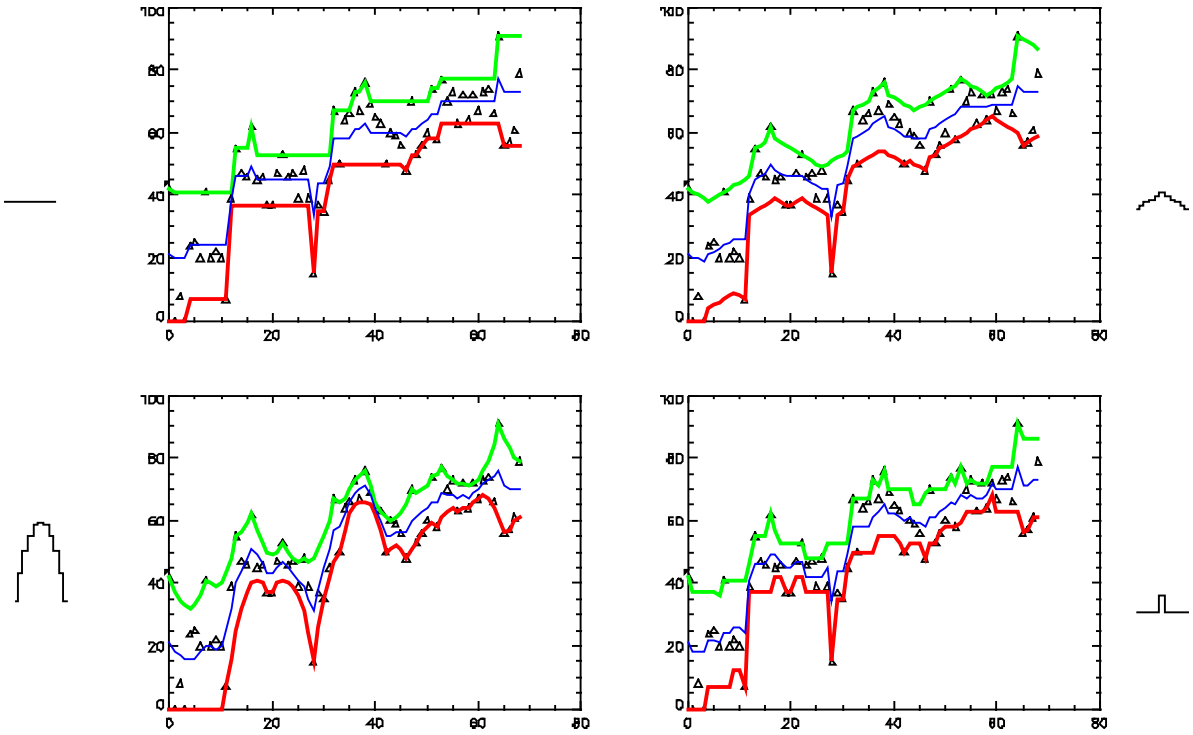

Fig. 5: Opening and closing with differently weighted structuring elements

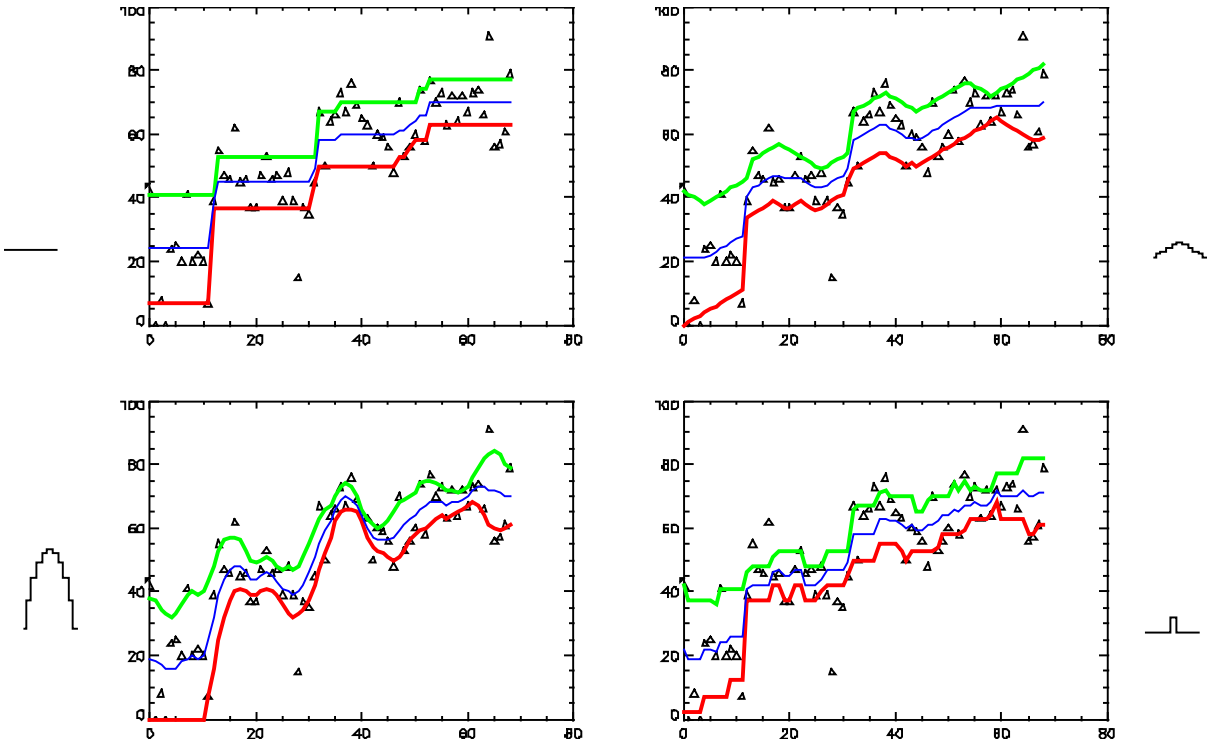

Fig 6: Openclose and closeopen on a function with differently weighted structuring elements (see text)